

Zero-Drift, Single-Supply, Rail-to-Rail Input/Output Operational Amplifier

FEATURES

- ▶ Lowest auto-zero amplifier noise
- ▶ Low offset voltage: 1 μV
- ▶ Input offset drift: 0.002 $\mu\text{V}/^\circ\text{C}$
- ▶ Rail-to-rail input and output swing
- ▶ 5 V single-supply operation
- ▶ High gain, CMRR, and PSRR: 130 dB
- ▶ Very low input bias current: 100 pA maximum
- ▶ Low supply current: 1.0 mA
- ▶ Overload recovery time: 50 μs
- ▶ No external components required
- ▶ Qualified for automotive applications

APPLICATIONS

- ▶ Automotive sensors
- ▶ Pressure and position sensors
- ▶ Strain gage amplifiers
- ▶ Medical instrumentation
- ▶ Thermocouple amplifiers
- ▶ Precision current sensing
- ▶ Photodiode amplifiers

GENERAL DESCRIPTION

This amplifier has ultralow offset, drift, and bias current. The AD8628/AD8629/AD8630 are wide bandwidth auto-zero amplifiers featuring rail-to-rail input and output swing and low noise. Operation is fully specified from 2.7 V to 5 V single supply ($\pm 1.35\text{ V}$ to $\pm 2.5\text{ V}$ dual supply).

The AD8628/AD8629/AD8630 provide benefits previously found only in expensive auto-zeroing or chopper-stabilized amplifiers. Using Analog Devices, Inc., topology, these zero-drift amplifiers combine low cost with high accuracy and low noise. No external capacitor is required. In addition, the AD8628/AD8629/AD8630 greatly reduce the digital switching noise found in most chopper-stabilized amplifiers.

With an offset voltage of only 1 μV , drift of less than 0.005 $\mu\text{V}/^\circ\text{C}$, and noise of only 0.5 μV p-p (0.1 Hz to 10 Hz), the AD8628/AD8629/AD8630 are suited for applications where error sources

PIN CONFIGURATIONS

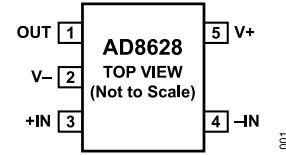


Figure 1. 5-Lead TSOT (UJ-5) and 5-Lead SOT-23 (RJ-5)

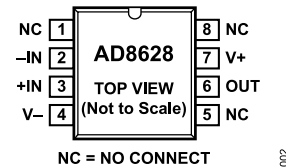


Figure 2. 8-Lead SOIC_N (R-8)

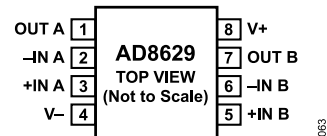


Figure 3. 8-Lead SOIC_N (R-8) and 8-Lead MSOP (RM-8)

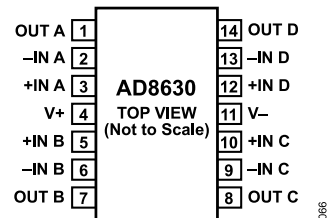


Figure 4. 14-Lead SOIC_N (R-14) and 14-Lead TSSOP (RU-14)

cannot be tolerated. Position and pressure sensors, medical equipment, and strain gage amplifiers benefit greatly from nearly zero drift over their operating temperature range. Many systems can take advantage of the rail-to-rail input and output swings provided by the AD8628/AD8629/AD8630 to reduce input biasing complexity and maximize SNR.

The AD8628/AD8629/AD8630 are specified for the extended industrial temperature range (-40°C to $+125^\circ\text{C}$). The AD8628 is available in [tiny 5-lead TSOT](#), [5-lead SOT-23](#), and [8-lead narrow SOIC plastic packages](#). The AD8629 is available in the [standard 8-lead narrow SOIC and MSOP plastic packages](#). The AD8630 quad amplifier is available in [14-lead narrow SOIC and 14-lead TSSOP plastic packages](#). See the [Ordering Guide](#) section for automotive grades.

Rev. M

DOCUMENT FEEDBACK

TECHNICAL SUPPORT

Information furnished by Analog Devices is believed to be accurate and reliable "as is". However, no responsibility is assumed by Analog Devices for its use, nor for any infringements of patents or other rights of third parties that may result from its use. Specifications subject to change without notice. No license is granted by implication or otherwise under any patent or patent rights of Analog Devices. Trademarks and registered trademarks are the property of their respective owners.

TABLE OF CONTENTS

Features.....	1	Noise Behavior with First-Order, Low-Pass Filter.....	15
Applications.....	1	Total Integrated Input-Referred Noise for First-Order Filter.....	15
Pin Configurations.....	1	Input Overvoltage Protection.....	15
General Description.....	1	Output Phase Reversal.....	16
Specifications.....	3	Overload Recovery Time.....	16
Electrical Characteristics— $V_S = 5.0\text{ V}$	3	Infrared Sensors.....	17
Electrical Characteristics— $V_S = 2.7\text{ V}$	4	Precision Current Shunt Sensor.....	17
Absolute Maximum Ratings.....	5	Output Amplifier for High Precision DACs.....	18
Thermal Characteristics.....	5	Outline Dimensions.....	19
ESD Caution.....	5	Ordering Guide.....	20
Typical Performance Characteristics.....	6	Automotive Products.....	21
Functional Description.....	14		
1/F Noise.....	14		
Peak-to-Peak Noise.....	14		

REVISION HISTORY**10/2022—Rev. L to Rev. M**

Change to Functional Description Section.....	14
---	----

SPECIFICATIONS

ELECTRICAL CHARACTERISTICS— $V_S = 5.0\text{ V}$

$V_S = 5.0\text{ V}$, $V_{CM} = 2.5\text{ V}$, $T_A = 25^\circ\text{C}$, unless otherwise noted.

Table 1.

Parameter	Symbol	Conditions	Min	Typ	Max	Unit
INPUT CHARACTERISTICS						
Offset Voltage	V_{OS}	$-40^\circ\text{C} \leq T_A \leq +125^\circ\text{C}$	1	5	5	μV
					10	μV
Input Bias Current	I_B	$-40^\circ\text{C} \leq T_A \leq +125^\circ\text{C}$	30	100	100	pA
			100	300	300	pA
Input Offset Current	I_{OS}	$-40^\circ\text{C} \leq T_A \leq +125^\circ\text{C}$	50	200	200	pA
					250	pA
Input Voltage Range			0		5	V
Common-Mode Rejection Ratio	CMRR	$V_{CM} = 0\text{ V to } 5\text{ V}$ $-40^\circ\text{C} \leq T_A \leq +125^\circ\text{C}$	120	140		dB
			115	130		dB
Large Signal Voltage Gain	A_{VO}	$R_L = 10\text{ k}\Omega$, $V_O = 0.3\text{ V to } 4.7\text{ V}$ $-40^\circ\text{C} \leq T_A \leq +125^\circ\text{C}$	125	145		dB
			120	135		dB
Offset Voltage Drift	$\Delta V_{OS}/\Delta T$	$-40^\circ\text{C} \leq T_A \leq +125^\circ\text{C}$	0.002	0.02	0.02	$\mu\text{V}/^\circ\text{C}$
OUTPUT CHARACTERISTICS						
Output Voltage High	V_{OH}	$R_L = 100\text{ k}\Omega$ to ground $-40^\circ\text{C} \leq T_A \leq +125^\circ\text{C}$	4.99	4.996		V
			4.99	4.995		V
			4.95	4.98		V
			4.95	4.97		V
Output Voltage Low	V_{OL}	$R_L = 100\text{ k}\Omega$ to V_+ $-40^\circ\text{C} \leq T_A \leq +125^\circ\text{C}$	1	5	5	mV
			2	5		mV
			10	20		mV
			15	20		mV
Short-Circuit Limit	I_{SC}	$-40^\circ\text{C} \leq T_A \leq +125^\circ\text{C}$	± 25	± 50		mA
				± 40		mA
Output Current	I_O	$-40^\circ\text{C} \leq T_A \leq +125^\circ\text{C}$	± 30			mA
				± 15		mA
POWER SUPPLY						
Power Supply Rejection Ratio	PSRR	$V_S = 2.7\text{ V to } 5.5\text{ V}$, $-40^\circ\text{C} \leq T_A \leq +125^\circ\text{C}$	115	130		dB
Supply Current per Amplifier	I_{SY}	$V_O = V_S/2$ $-40^\circ\text{C} \leq T_A \leq +125^\circ\text{C}$	0.85	1.1	1.1	mA
			1.0	1.2	1.2	mA
INPUT CAPACITANCE						
Differential	C_{IN}			1.5		pF
Common Mode				8.0		pF
DYNAMIC PERFORMANCE						
Slew Rate	SR	$R_L = 10\text{ k}\Omega$		1.0		$\text{V}/\mu\text{s}$
Overload Recovery Time				0.05		ms
Gain Bandwidth Product	GBP			2.5		MHz
NOISE PERFORMANCE						
Voltage Noise	e_n p-p	0.1 Hz to 10 Hz		0.5		$\mu\text{V p-p}$
				0.16		$\mu\text{V p-p}$
Voltage Noise Density	e_n	$f = 1\text{ kHz}$		22		$\text{nV}/\sqrt{\text{Hz}}$
Current Noise Density	i_n	$f = 10\text{ Hz}$		5		$\text{fA}/\sqrt{\text{Hz}}$

SPECIFICATIONS

ELECTRICAL CHARACTERISTICS— $V_S = 2.7\text{ V}$

$V_S = 2.7\text{ V}$, $V_{CM} = 1.35\text{ V}$, $T_A = 25^\circ\text{C}$, unless otherwise noted.

Table 2.

Parameter	Symbol	Conditions	Min	Typ	Max	Unit
INPUT CHARACTERISTICS						
Offset Voltage	V_{OS}	$-40^\circ\text{C} \leq T_A \leq +125^\circ\text{C}$	1	5	5	μV
					10	μV
Input Bias Current	I_B	$-40^\circ\text{C} \leq T_A \leq +125^\circ\text{C}$	30	100		pA
			100	300		pA
Input Offset Current	I_{OS}	$-40^\circ\text{C} \leq T_A \leq +125^\circ\text{C}$	1.0	1.5		nA
			50	200		pA
Input Voltage Range		$-40^\circ\text{C} \leq T_A \leq +125^\circ\text{C}$			250	pA
Input Voltage Range		$-40^\circ\text{C} \leq T_A \leq +125^\circ\text{C}$	0		2.7	V
Common-Mode Rejection Ratio	CMRR	$V_{CM} = 0\text{ V to } 2.7\text{ V}$ $-40^\circ\text{C} \leq T_A \leq +125^\circ\text{C}$	115	130		dB
			110	120		dB
Large Signal Voltage Gain	A_{VO}	$R_L = 10\text{ k}\Omega$, $V_O = 0.3\text{ V to } 2.4\text{ V}$ $-40^\circ\text{C} \leq T_A \leq +125^\circ\text{C}$	110	140		dB
			105	130		dB
Offset Voltage Drift	$\Delta V_{OS}/\Delta T$	$-40^\circ\text{C} \leq T_A \leq +125^\circ\text{C}$		0.002	0.02	$\mu\text{V}/^\circ\text{C}$
OUTPUT CHARACTERISTICS						
Output Voltage High	V_{OH}	$R_L = 100\text{ k}\Omega$ to ground $-40^\circ\text{C} \leq T_A \leq +125^\circ\text{C}$	2.68	2.695		V
			2.68	2.695		V
			2.67	2.68		V
			2.67	2.675		V
Output Voltage Low	V_{OL}	$R_L = 100\text{ k}\Omega$ to V_+ $-40^\circ\text{C} \leq T_A \leq +125^\circ\text{C}$	1	5		mV
			2	5		mV
			10	20		mV
			15	20		mV
Short-Circuit Limit	I_{SC}	$-40^\circ\text{C} \leq T_A \leq +125^\circ\text{C}$	± 10	± 15		mA
				± 10		mA
Output Current	I_O	$-40^\circ\text{C} \leq T_A \leq +125^\circ\text{C}$	± 10			mA
			± 5			mA
POWER SUPPLY						
Power Supply Rejection Ratio	PSRR	$V_S = 2.7\text{ V to } 5.5\text{ V}$, $-40^\circ\text{C} \leq T_A \leq +125^\circ\text{C}$	115	130		dB
Supply Current per Amplifier	I_{SY}	$V_O = V_S/2$ $-40^\circ\text{C} \leq T_A \leq +125^\circ\text{C}$	0.75	1.0		mA
			0.9	1.2		mA
INPUT CAPACITANCE						
Differential	C_{IN}			1.5		pF
Common Mode				8.0		pF
DYNAMIC PERFORMANCE						
Slew Rate	SR	$R_L = 10\text{ k}\Omega$		1		$\text{V}/\mu\text{s}$
Overload Recovery Time				0.05		ms
Gain Bandwidth Product	GBP			2		MHz
NOISE PERFORMANCE						
Voltage Noise	e_n p-p	0.1 Hz to 10 Hz		0.5		$\mu\text{V p-p}$
Voltage Noise Density	e_n	$f = 1\text{ kHz}$		22		$\text{nV}/\sqrt{\text{Hz}}$
Current Noise Density	i_n	$f = 10\text{ Hz}$		5		$\text{fA}/\sqrt{\text{Hz}}$

ABSOLUTE MAXIMUM RATINGS

Table 3.

Parameter	Rating
Supply Voltage	6 V
Input Voltage	GND – 0.3 V to $V_S + 0.3$ V
Differential Input Voltage ¹	±5.0 V
Output Short-Circuit Duration to GND	Indefinite
Storage Temperature Range	–65°C to +150°C
Operating Temperature Range	–40°C to +125°C
Junction Temperature Range	–65°C to +150°C
Lead Temperature (Soldering, 60 sec)	300°C
ESD AD8628	
HBM 8-Lead SOIC	±7000V
FICDM 8-Lead SOIC	±1500V
FICDM 5-Lead TSOT	±1000V
MM 8-Lead SOIC	±200V
ESD AD8629	
HBM 8-Lead SOIC	±4000V
FICDM 8-Lead SOIC	±1000V
ESD AD8630	
HBM 14-Lead SOIC	±5000V
FICDM 14-Lead SOIC	±1500V
FICDM 14-Lead TSSOP	±1500V
MM 14-Lead SOIC	±200V

¹ Differential input voltage is limited to ±5 V or the supply voltage, whichever is less.

Stresses at or above those listed under Absolute Maximum Ratings may cause permanent damage to the product. This is a stress

rating only; functional operation of the product at these or any other conditions above those indicated in the operational section of this specification is not implied. Operation beyond the maximum operating conditions for extended periods may affect product reliability.

THERMAL CHARACTERISTICS

θ_{JA} is specified for worst-case conditions, that is, θ_{JA} is specified for the device soldered in a circuit board for surface-mount packages. This was measured using a standard two-layer board.

Table 4.

Package Type	θ_{JA}	θ_{JC}	Unit
5-Lead TSOT (UJ-5)	207	61	°C/W
5-Lead SOT-23 (RJ-5)	230	146	°C/W
8-Lead SOIC_N (R-8)	158	43	°C/W
8-Lead MSOP (RM-8)	190	44	°C/W
14-Lead SOIC_N (R-14)	105	43	°C/W
14-Lead TSSOP (RU-14)	148	23	°C/W

ESD CAUTION



ESD (electrostatic discharge) sensitive device. Charged devices and circuit boards can discharge without detection. Although this product features patented or proprietary protection circuitry, damage may occur on devices subjected to high energy ESD. Therefore, proper ESD precautions should be taken to avoid performance degradation or loss of functionality.

TYPICAL PERFORMANCE CHARACTERISTICS

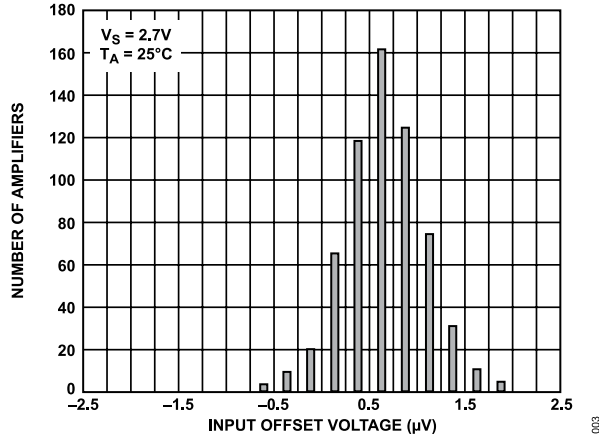


Figure 5. Input Offset Voltage Distribution

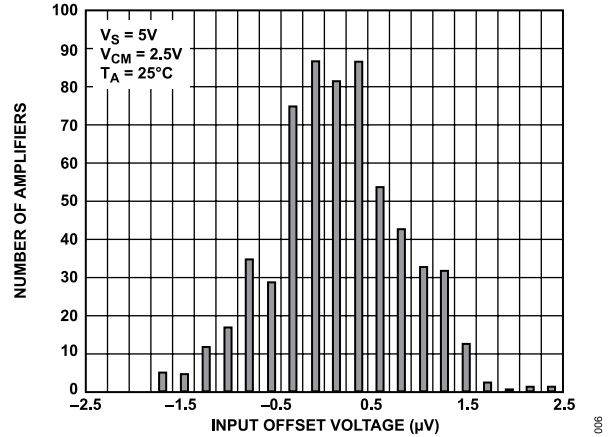


Figure 8. Input Offset Voltage Distribution

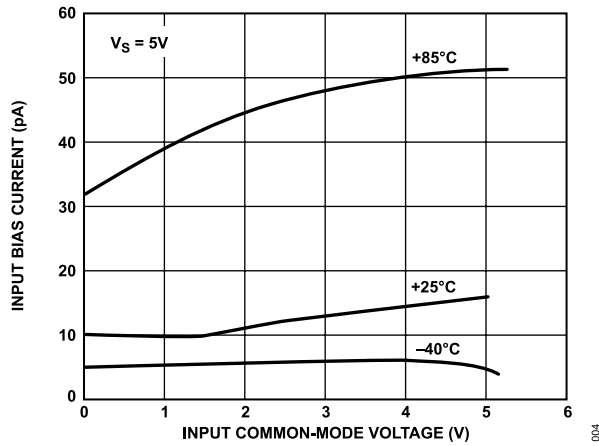


Figure 6. AD8628 Input Bias Current vs. Input Common-Mode Voltage

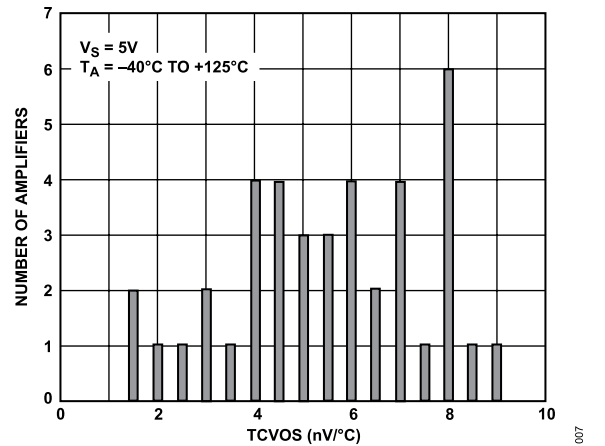


Figure 9. Input Offset Voltage Drift

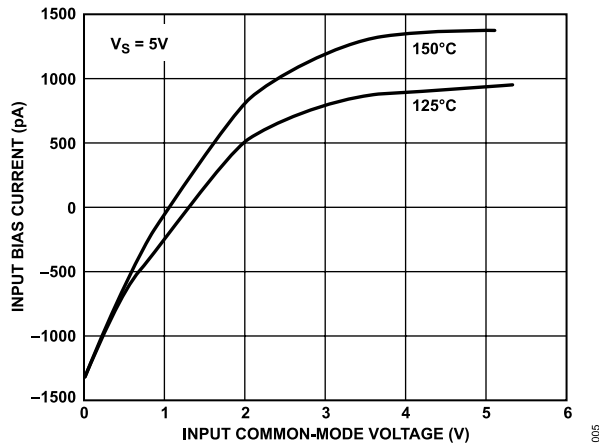


Figure 7. AD8628 Input Bias Current vs. Input Common-Mode Voltage

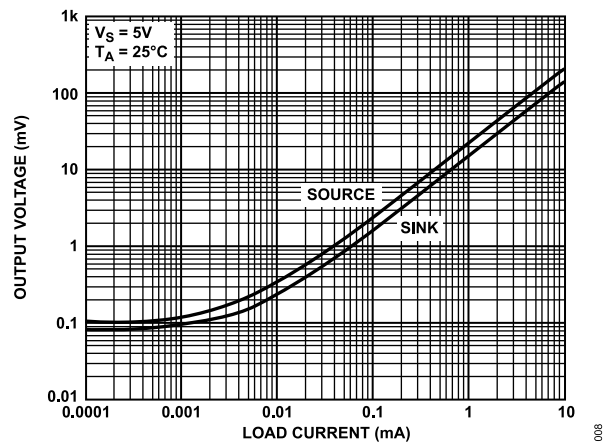


Figure 10. Output Voltage to Supply Rail vs. Load Current

TYPICAL PERFORMANCE CHARACTERISTICS

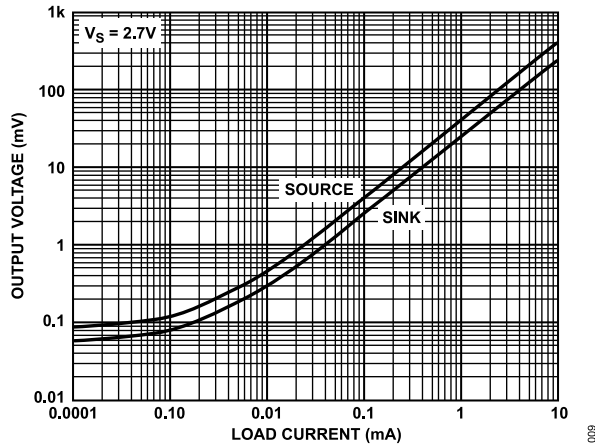


Figure 11. Output Voltage to Supply Rail vs. Load Current

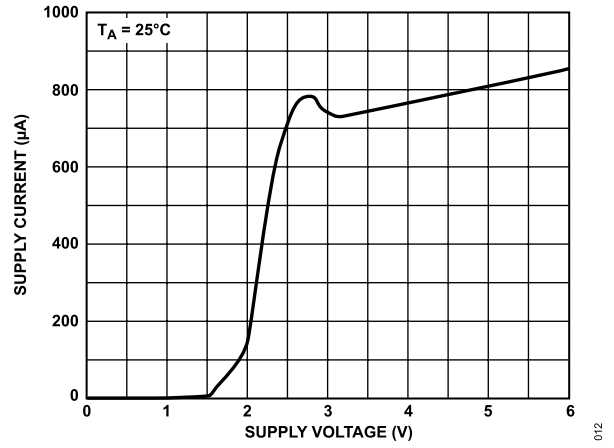


Figure 14. Supply Current vs. Supply Voltage

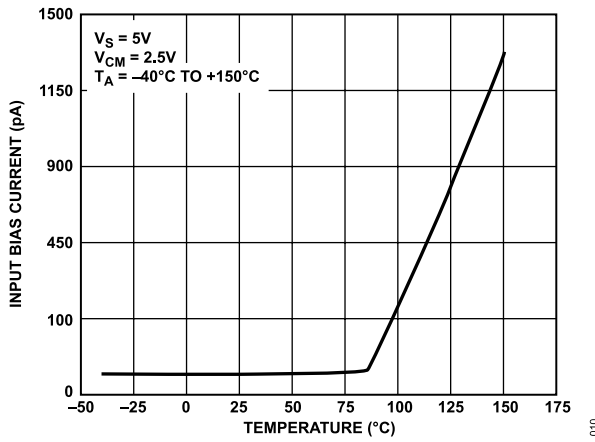


Figure 12. AD8628 Input Bias Current vs. Temperature

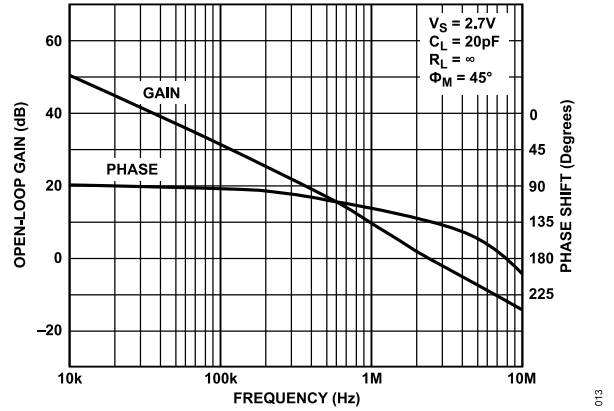


Figure 15. Open-Loop Gain and Phase vs. Frequency

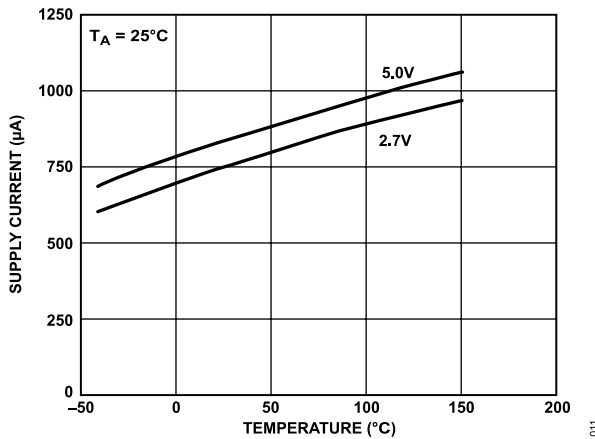


Figure 13. Supply Current vs. Temperature

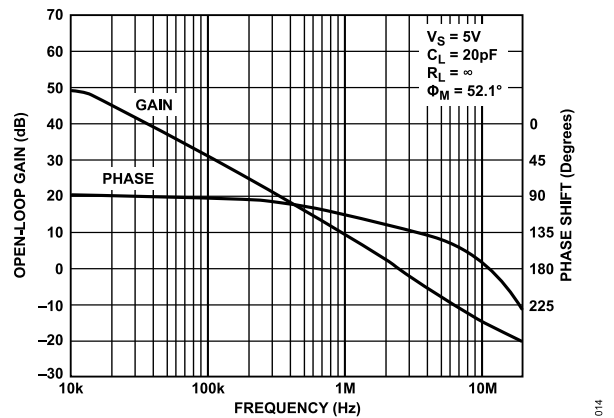


Figure 16. Open-Loop Gain and Phase vs. Frequency

TYPICAL PERFORMANCE CHARACTERISTICS

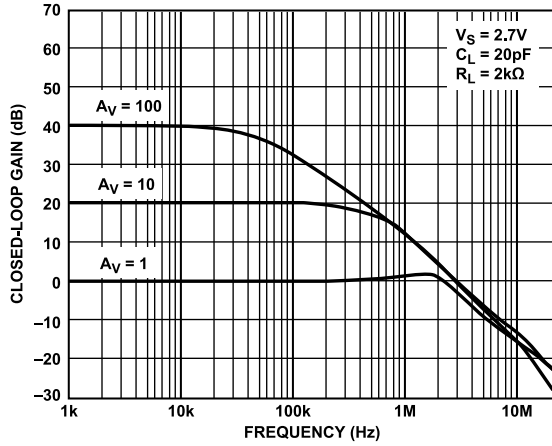


Figure 17. Closed-Loop Gain vs. Frequency

015

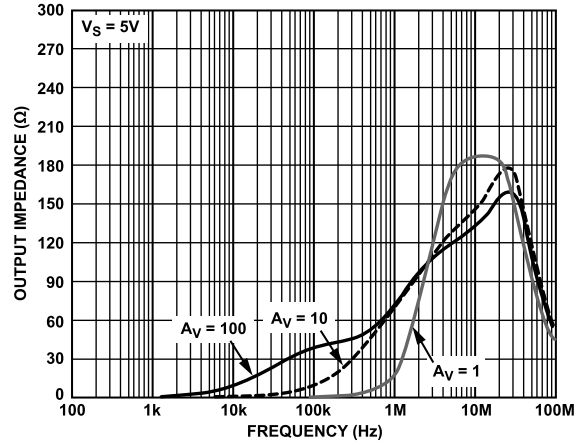


Figure 20. Output Impedance vs. Frequency

018

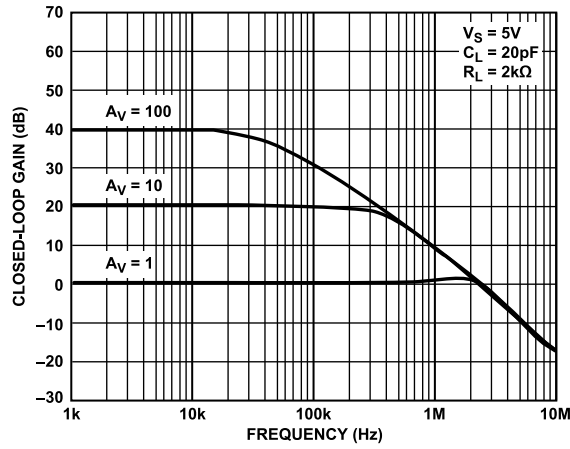


Figure 18. Closed-Loop Gain vs. Frequency

016

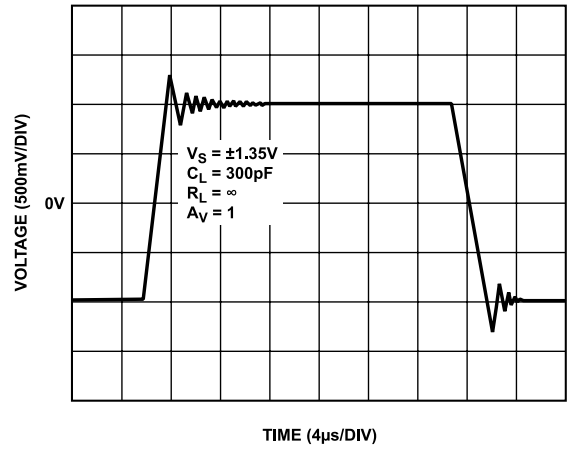


Figure 21. Large Signal Transient Response

019

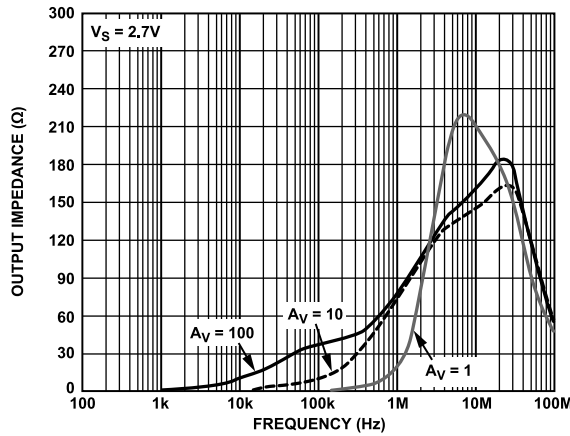


Figure 19. Output Impedance vs. Frequency

017

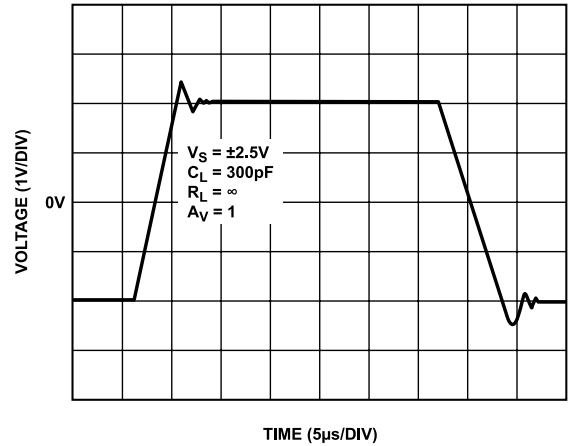


Figure 22. Large Signal Transient Response

020

TYPICAL PERFORMANCE CHARACTERISTICS

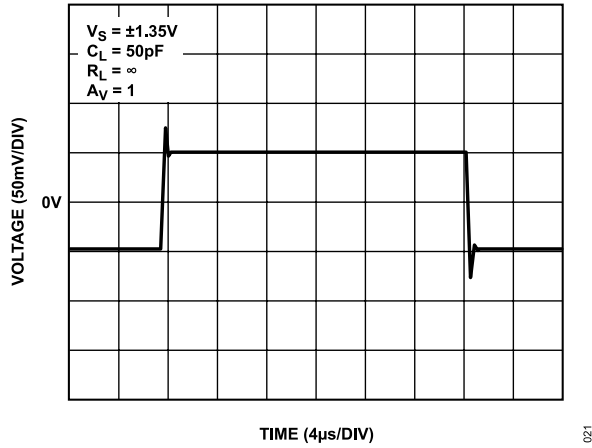


Figure 23. Small Signal Transient Response

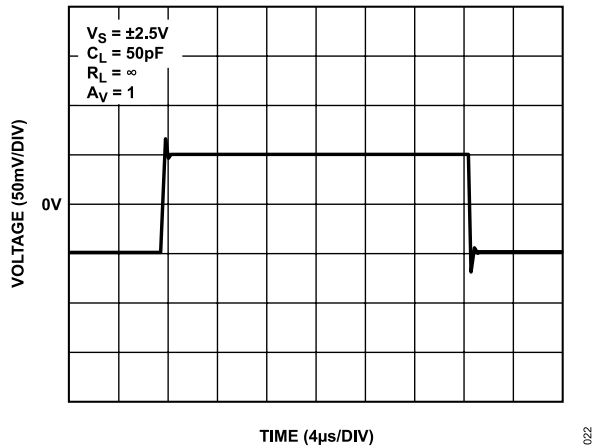


Figure 24. Small Signal Transient Response

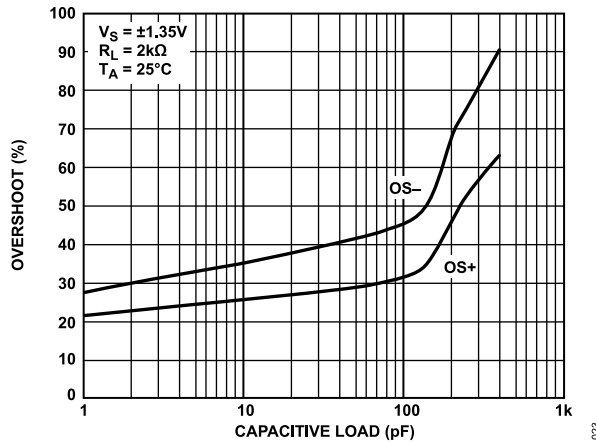


Figure 25. Small Signal Overshoot vs. Load Capacitance

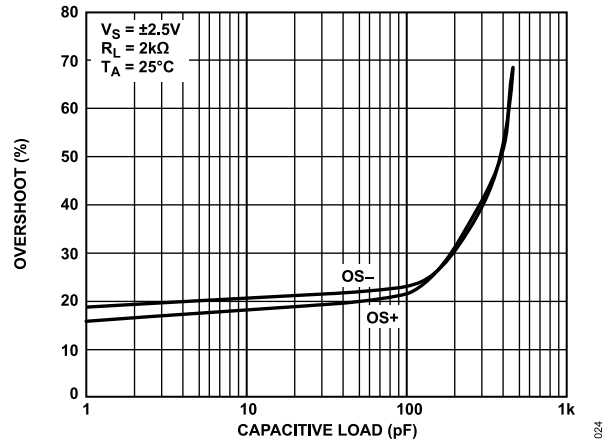


Figure 26. Small Signal Overshoot vs. Load Capacitance

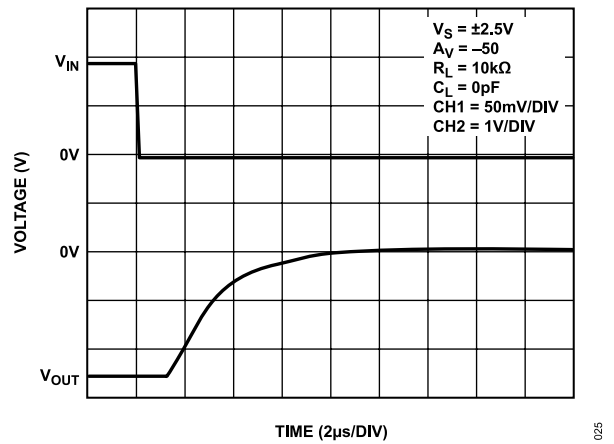


Figure 27. Positive Overvoltage Recovery

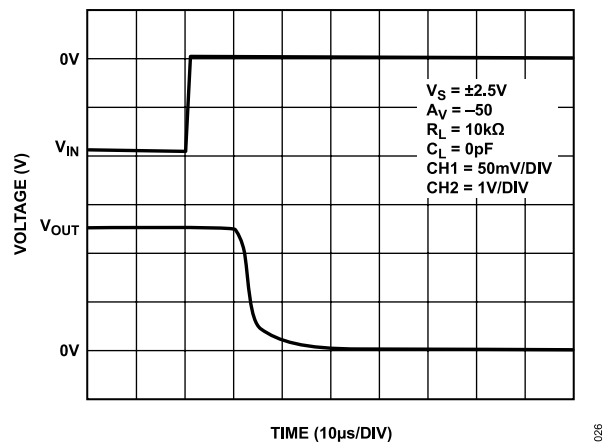


Figure 28. Negative Overvoltage Recovery

TYPICAL PERFORMANCE CHARACTERISTICS

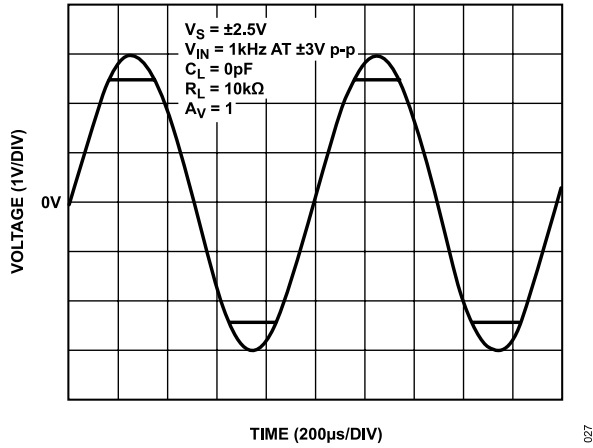


Figure 29. No Phase Reversal

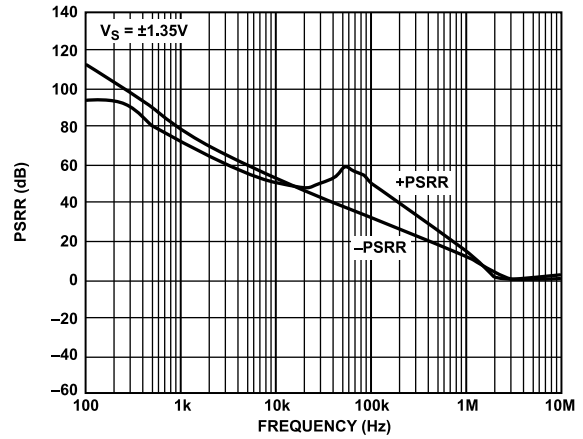


Figure 32. PSRR vs. Frequency

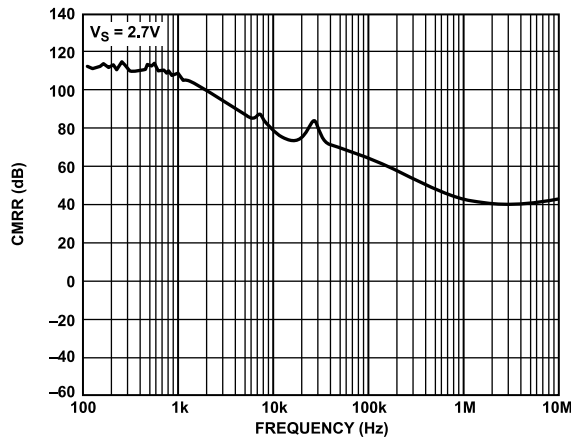


Figure 30. CMRR vs. Frequency

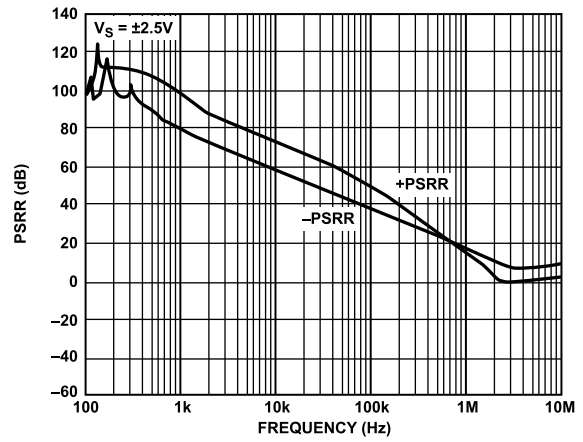


Figure 33. PSRR vs. Frequency

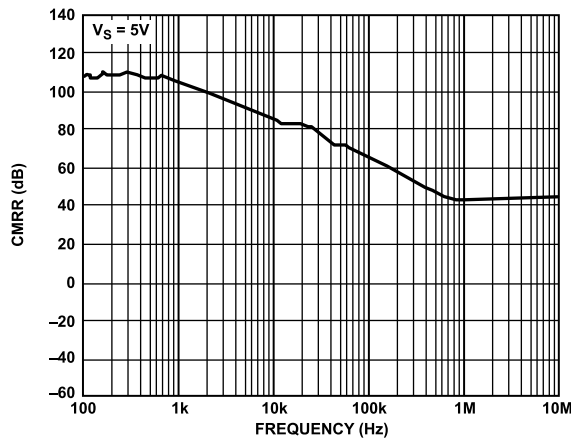


Figure 31. CMRR vs. Frequency

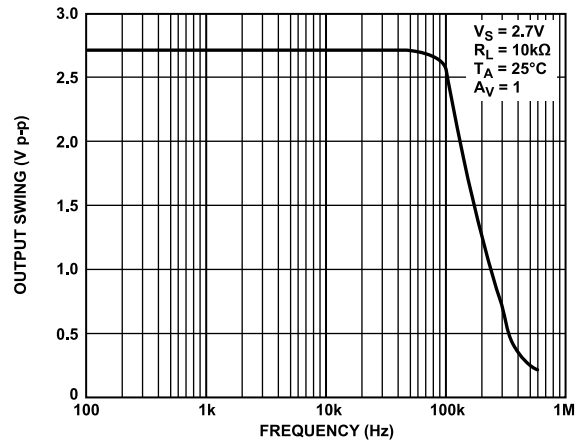


Figure 34. Maximum Output Swing vs. Frequency

TYPICAL PERFORMANCE CHARACTERISTICS

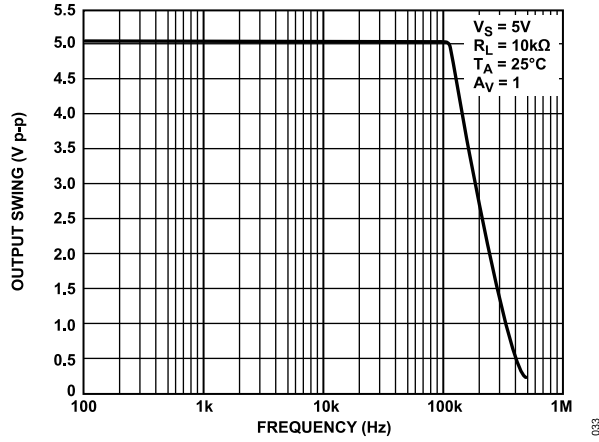


Figure 35. Maximum Output Swing vs. Frequency

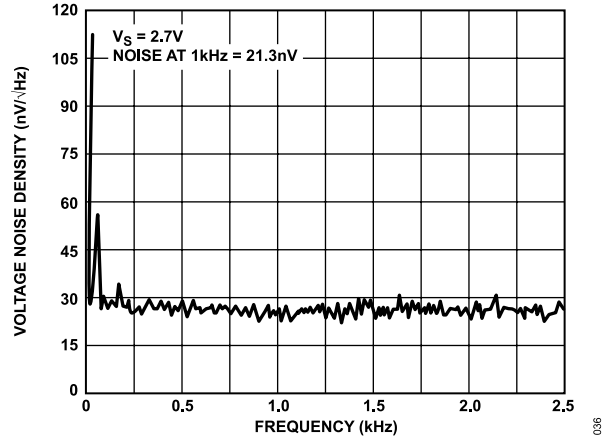


Figure 38. Voltage Noise Density at 2.7 V from 0 Hz to 2.5 kHz

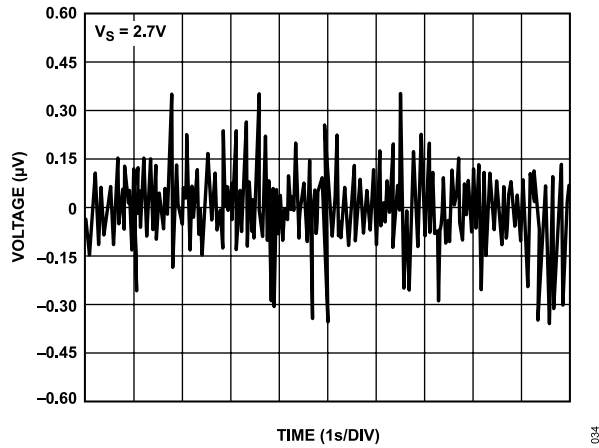


Figure 36. 0.1 Hz to 10 Hz Noise

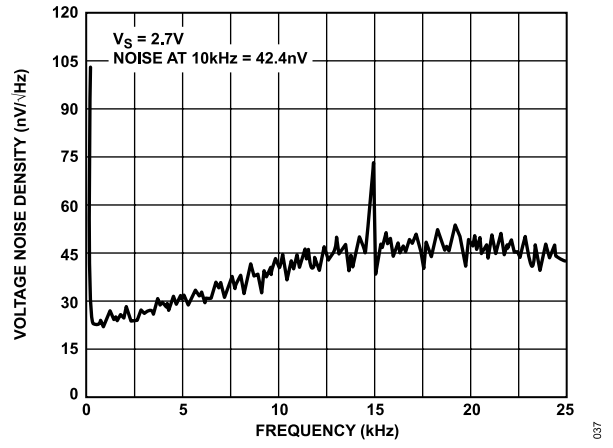


Figure 39. Voltage Noise Density at 2.7 V from 0 Hz to 25 kHz

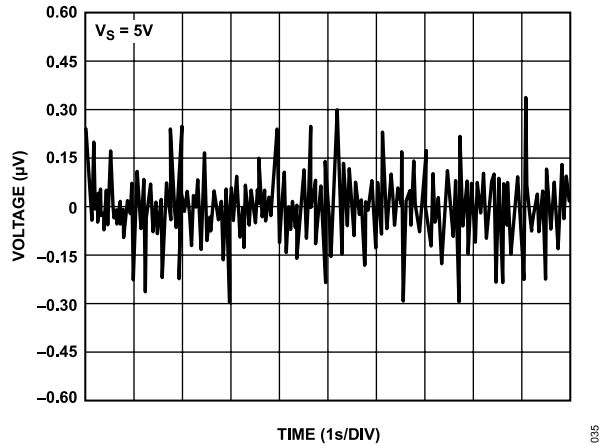


Figure 37. 0.1 Hz to 10 Hz Noise

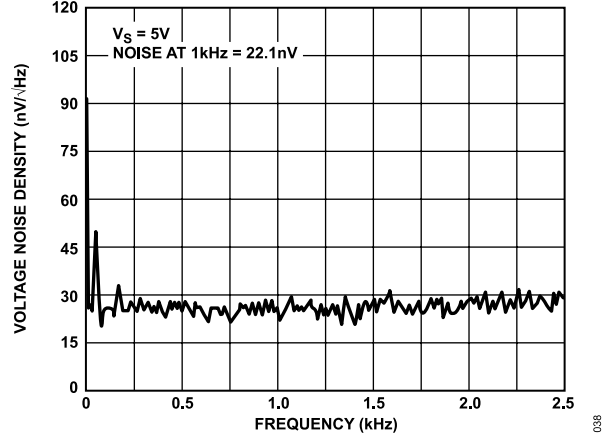


Figure 40. Voltage Noise Density at 5 V from 0 Hz to 2.5 kHz

TYPICAL PERFORMANCE CHARACTERISTICS

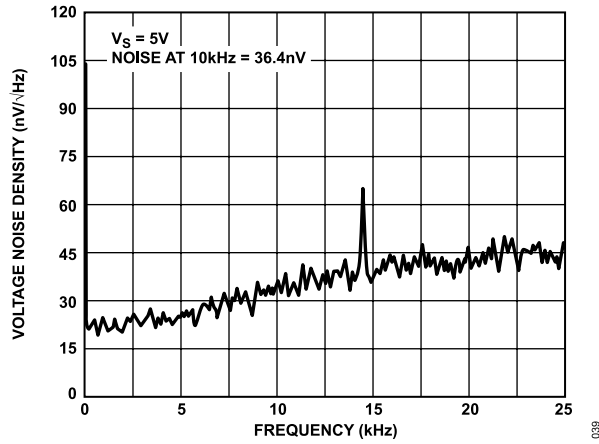


Figure 41. Voltage Noise Density at 5 V from 0 Hz to 25 kHz

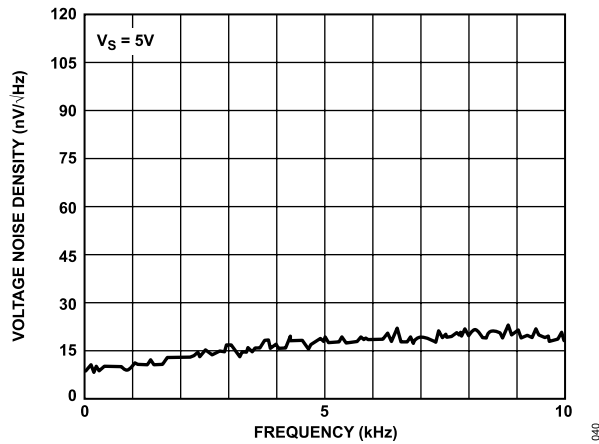


Figure 42. Voltage Noise Density at 5 V from 0 Hz to 10 kHz

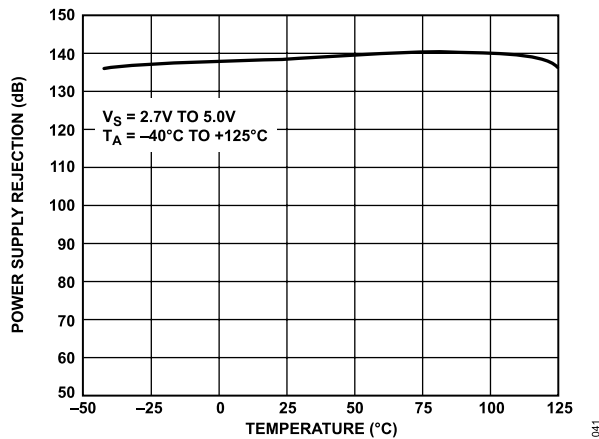


Figure 43. Power Supply Rejection vs. Temperature

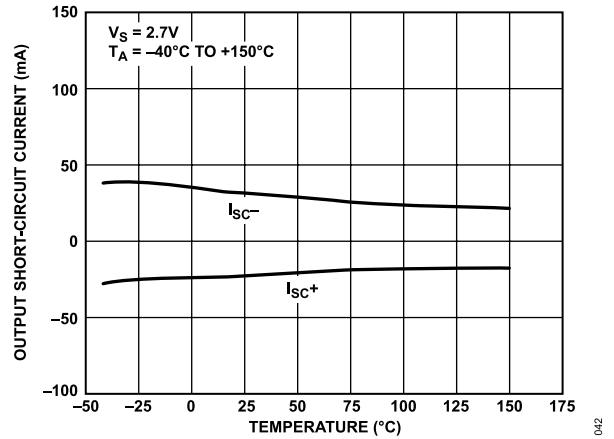


Figure 44. Output Short-Circuit Current vs. Temperature

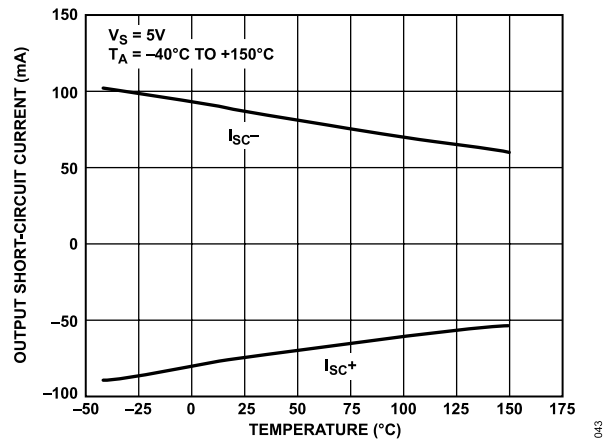


Figure 45. Output Short-Circuit Current vs. Temperature

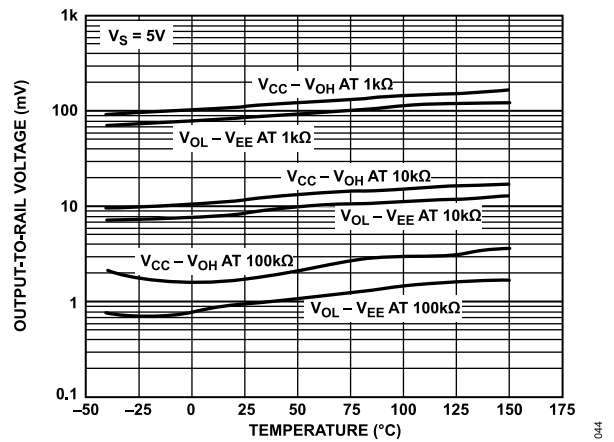


Figure 46. Output-to-Rail Voltage vs. Temperature

TYPICAL PERFORMANCE CHARACTERISTICS

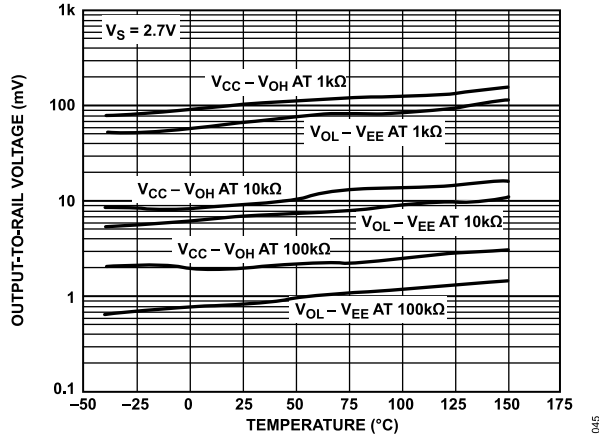


Figure 47. Output-to-Rail Voltage vs. Temperature

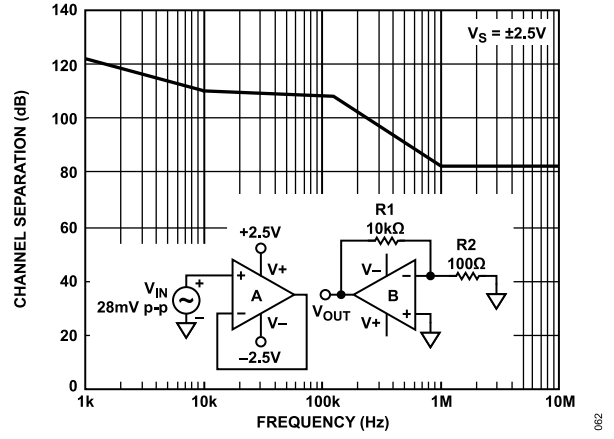


Figure 48. AD8629/AD8630 Channel Separation vs. Frequency

FUNCTIONAL DESCRIPTION

The AD8628/AD8629/AD8630 are single-supply, ultrahigh precision rail-to-rail input and output operational amplifiers. The typical offset voltage of less than 1 μV allows these amplifiers to be easily configured for high gains without risk of excessive output voltage errors. The extremely small temperature drift of 2 $\text{nV}/^\circ\text{C}$ ensures a minimum offset voltage error over their entire temperature range of -40°C to $+125^\circ\text{C}$, making these amplifiers ideal for a variety of sensitive measurement applications in harsh operating environments.

The AD8628/AD8629/AD8630 achieve a high degree of precision through a patented combination of auto-zeroing and chopping. This unique topology allows the AD8628/AD8629/AD8630 to maintain their low offset voltage over a wide temperature range and over their operating lifetime. The AD8628/AD8629/AD8630 also optimize the noise and bandwidth over previous generations of auto-zero amplifiers, offering the lowest voltage noise of any auto-zero amplifier by more than 50%.

Previous designs used either auto-zeroing or chopping to add precision to the specifications of an amplifier. Auto-zeroing results in low noise energy at the auto-zeroing frequency, at the expense of higher low frequency noise due to aliasing of wideband noise into the auto-zeroed frequency band. Chopping results in lower low frequency noise at the expense of larger noise energy at the chopping frequency. The AD8628/AD8629/AD8630 family uses both auto-zeroing and chopping in a patented ping-pong arrangement to obtain lower low frequency noise together with lower energy at the chopping and auto-zeroing frequencies, maximizing the signal-to-noise ratio for the majority of applications without the need for additional filtering. The relatively high clock frequency of 15 kHz simplifies filter requirements for a wide, useful noise-free bandwidth.

The AD8628 is among the few auto-zero amplifiers offered in the 5-lead TSOT package. This provides a significant improvement over the ac parameters of the previous auto-zero amplifiers. The AD8628/AD8629/AD8630 have low noise over a relatively wide bandwidth (0.1 Hz to 10 kHz) and can be used where the highest dc precision is required. In systems with signal bandwidths of from 5 kHz to 10 kHz, the AD8628/AD8629/AD8630 provide true 16-bit accuracy, making them the best choice for very high resolution systems.

1/F NOISE

1/f noise, also known as pink noise, is a major contributor to errors in dc-coupled measurements. This 1/f noise error term can be in the range of several μV or more, and, when amplified with the closed-loop gain of the circuit, can show up as a large output offset. For example, when an amplifier with a 5 μV p-p 1/f noise is configured for a gain of 1000, its output has 5 mV of error due to the 1/f noise. However, the AD8628/AD8629/AD8630 eliminate 1/f noise internally, thereby greatly reducing output errors.

The internal elimination of 1/f noise is accomplished as follows. 1/f noise appears as a slowly varying offset to the AD8628/AD8629/AD8630 inputs. Auto-zeroing corrects any dc or low frequency

offset. Therefore, the 1/f noise component is essentially removed, leaving the AD8628/AD8629/AD8630 free of 1/f noise.

One advantage that the AD8628/AD8629/AD8630 bring to system applications over competitive auto-zero amplifiers is their very low noise. The comparison shown in Figure 49 indicates an input-referred noise density of 19.4 $\text{nV}/\sqrt{\text{Hz}}$ at 1 kHz for the AD8628, which is much better than the Competitor A and Competitor B. The noise is flat from dc to 1.5 kHz, slowly increasing up to 20 kHz. The lower noise at low frequency is desirable where auto-zero amplifiers are widely used.

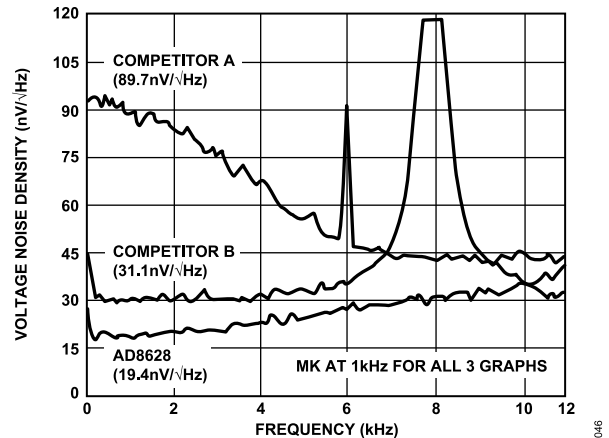


Figure 49. Noise Spectral Density of AD8628 vs. Competition

PEAK-TO-PEAK NOISE

Because of the ping-pong action between auto-zeroing and chopping, the peak-to-peak noise of the AD8628/AD8629/AD8630 is much lower than the competition. Figure 50 and Figure 51 show this comparison.

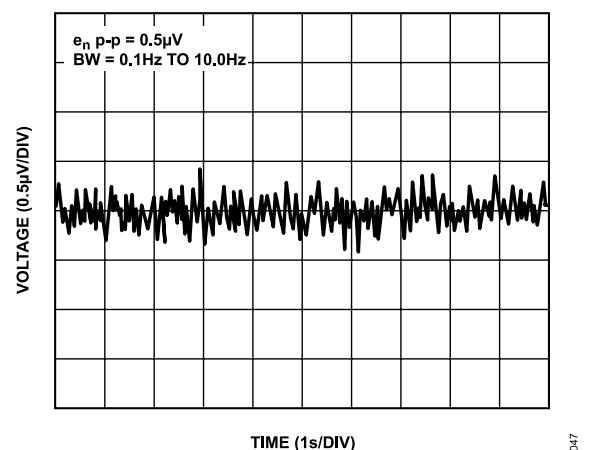


Figure 50. AD8628 Peak-to-Peak Noise

FUNCTIONAL DESCRIPTION

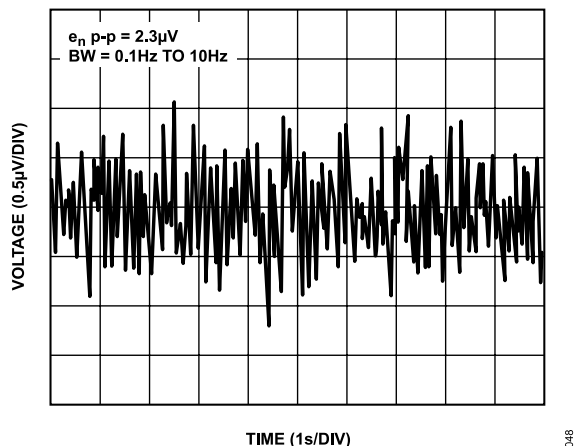


Figure 51. Competitor A Peak-to-Peak Noise

NOISE BEHAVIOR WITH FIRST-ORDER, LOW-PASS FILTER

The AD8628 was simulated as a low-pass filter (see Figure 53) and then configured as shown in Figure 52. The behavior of the AD8628 matches the simulated data. It was verified that noise is rolled off by first-order filtering. Figure 53 and Figure 54 show the difference between the simulated and actual transfer functions of the circuit shown in Figure 52.

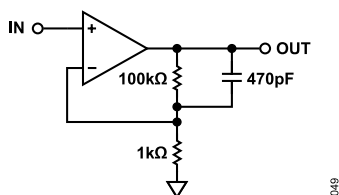


Figure 52. First-Order Low-Pass Filter Test Circuit, $\times 101$ Gain and 3 kHz Corner Frequency

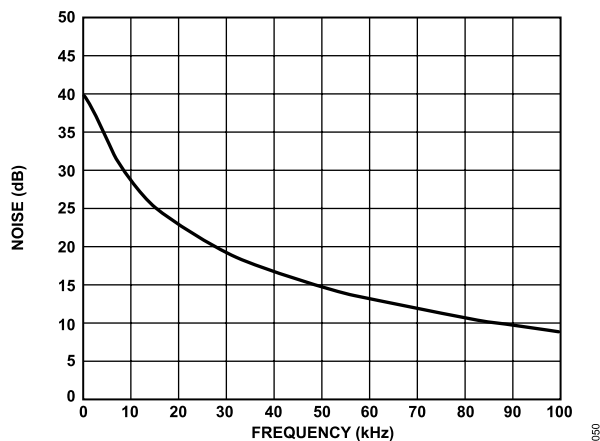


Figure 53. Simulation Transfer Function of the Test Circuit in Figure 52

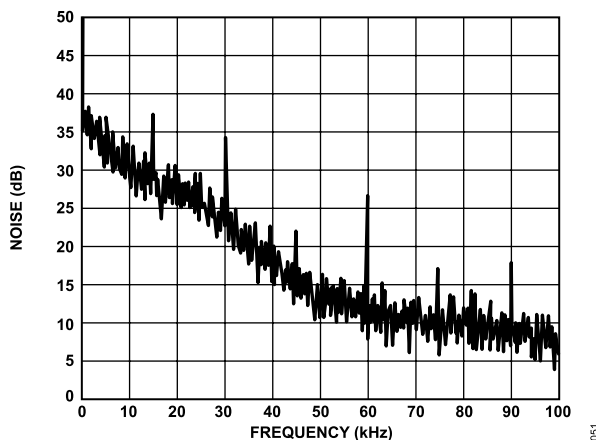


Figure 54. Actual Transfer Function of the Test Circuit in Figure 52

The measured noise spectrum of the test circuit charted in Figure 54 shows that noise between 5 kHz and 45 kHz is successfully rolled off by the first-order filter.

TOTAL INTEGRATED INPUT-REFERRED NOISE FOR FIRST-ORDER FILTER

For a first-order filter, the total integrated noise from the AD8628 is lower than the noise of Competitor A.

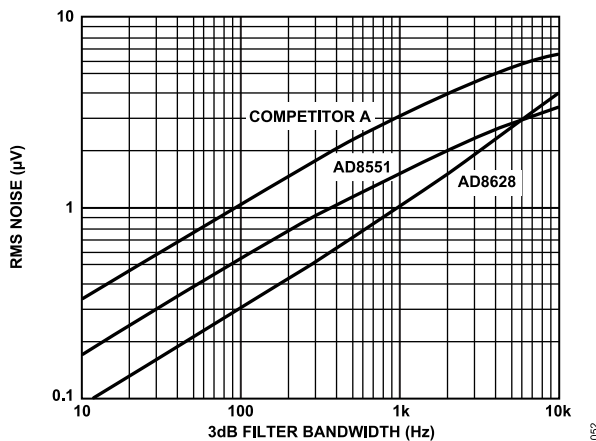


Figure 55. RMS Noise vs. 3 dB Filter Bandwidth in Hz

INPUT OVERVOLTAGE PROTECTION

Although the AD8628/AD8629/AD8630 are rail-to-rail input amplifiers, care should be taken to ensure that the potential difference between the inputs does not exceed the supply voltage. Under normal negative feedback operating conditions, the amplifier corrects its output to ensure that the two inputs are at the same voltage. However, if either input exceeds either supply rail by more than 0.3 V, large currents begin to flow through the ESD protection diodes in the amplifier.

These diodes are connected between the inputs and each supply rail to protect the input transistors against an electrostatic discharge event, and they are normally reverse-biased. However, if the input

FUNCTIONAL DESCRIPTION

voltage exceeds the supply voltage, these ESD diodes can become forward-biased. Without current limiting, excessive amounts of current could flow through these diodes, causing permanent damage to the device. If inputs are subject to overvoltage, appropriate series resistors should be inserted to limit the diode current to less than 5 mA maximum.

OUTPUT PHASE REVERSAL

Output phase reversal occurs in some amplifiers when the input common-mode voltage range is exceeded. As common-mode voltage is moved outside the common-mode range, the outputs of these amplifiers can suddenly jump in the opposite direction to the supply rail. This is the result of the differential input pair shutting down, causing a radical shifting of internal voltages that results in the erratic output behavior.

The AD8628/AD8629/AD8630 amplifiers have been carefully designed to prevent any output phase reversal, provided that both inputs are maintained within the supply voltages. If one or both inputs could exceed either supply voltage, a resistor should be placed in series with the input to limit the current to less than 5 mA. This ensures that the output does not reverse its phase.

OVERLOAD RECOVERY TIME

Many auto-zero amplifiers are plagued by a long overload recovery time, often in ms, due to the complicated settling behavior of the internal nulling loops after saturation of the outputs. The AD8628/AD8629/AD8630 have been designed so that internal settling occurs within two clock cycles after output saturation occurs. This results in a much shorter recovery time, less than 10 μ s, when compared to other auto-zero amplifiers. The wide bandwidth of the AD8628/AD8629/AD8630 enhances performance when the parts are used to drive loads that inject transients into the outputs. This is a common situation when an amplifier is used to drive the input of switched capacitor ADCs.

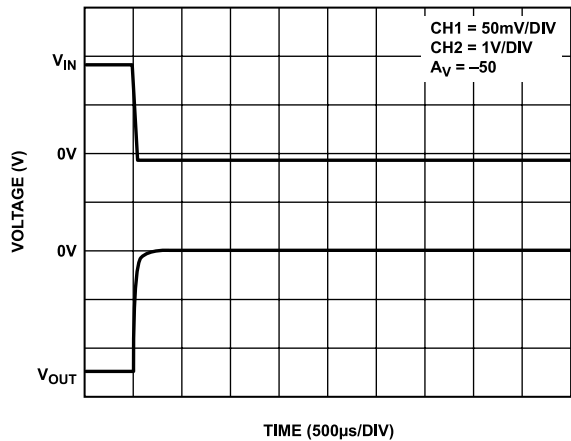


Figure 56. Positive Input Overload Recovery for the AD8628

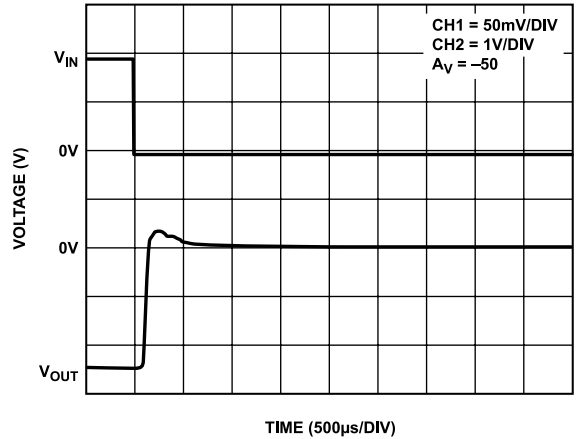


Figure 57. Positive Input Overload Recovery for Competitor A

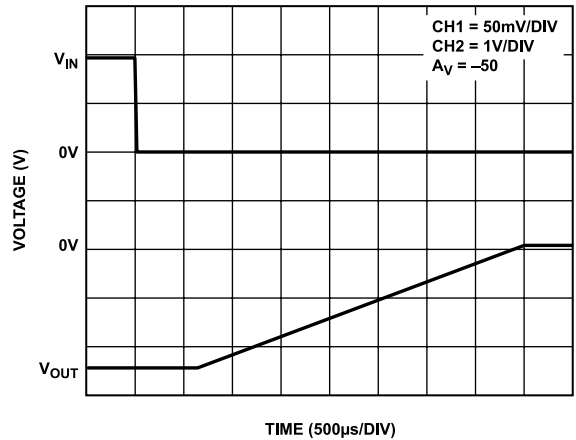


Figure 58. Positive Input Overload Recovery for Competitor B

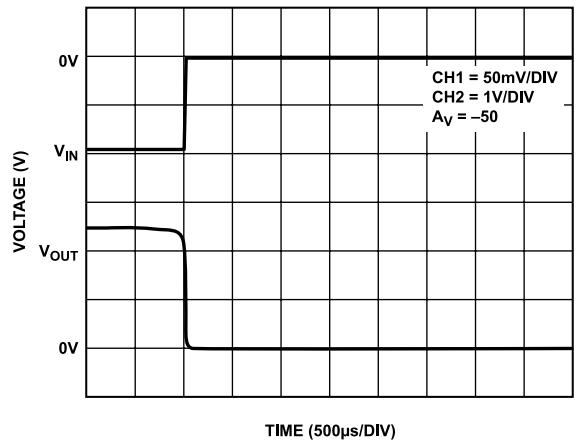


Figure 59. Negative Input Overload Recovery for the AD8628

FUNCTIONAL DESCRIPTION

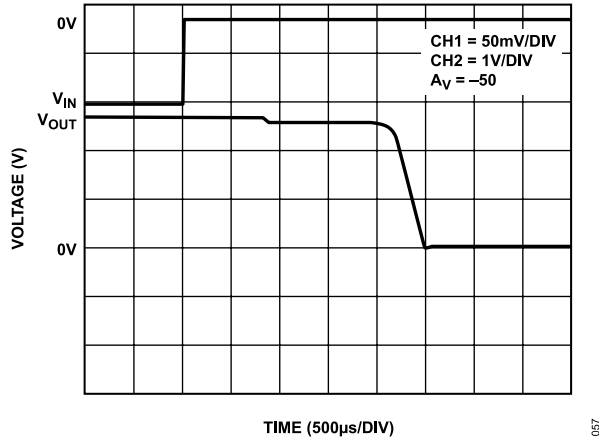


Figure 60. Negative Input Overload Recovery for Competitor A

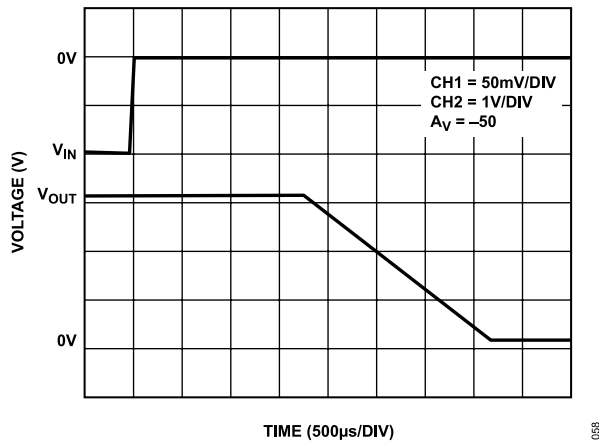


Figure 61. Negative Input Overload Recovery for Competitor B

The results shown in Figure 56 to Figure 61 are summarized in Table 5.

Table 5. Overload Recovery Time

Model	Positive Overload Recovery (μs)	Negative Overload Recovery (μs)
AD8628	6	9
Competitor A	650	25,000
Competitor B	40,000	35,000

INFRARED SENSORS

Infrared (IR) sensors, particularly thermopiles, are increasingly being used in temperature measurement for applications as wide ranging as automotive climate control, human ear thermometers, home insulation analysis, and automotive repair diagnostics. The relatively small output signal of the sensor demands high gain with very low offset voltage and drift to avoid dc errors.

If interstage ac coupling is used, as in Figure 62, low offset and drift prevent the output of the input amplifier from drifting close to saturation. The low input bias currents generate minimal errors from the output impedance of the sensor. As with pressure sensors,

the very low amplifier drift with time and temperature eliminate additional errors once the temperature measurement is calibrated. The low 1/f noise improves SNR for dc measurements taken over periods often exceeding one-fifth of a second.

Figure 62 shows a circuit that can amplify ac signals from 100 μV to 300 μV up to the 1 V to 3 V levels, with a gain of 10,000 for accurate analog-to-digital conversion.

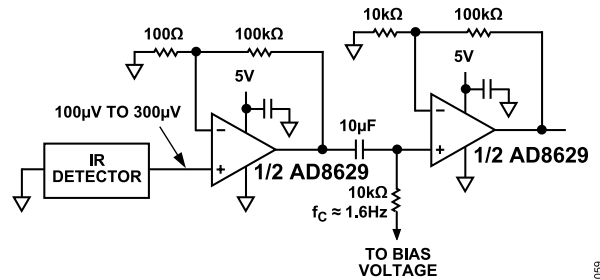


Figure 62. AD8629 Used as Preamp for Thermopile

PRECISION CURRENT SHUNT SENSOR

A precision current shunt sensor benefits from the unique attributes of auto-zero amplifiers when used in a differencing configuration, as shown in Figure 63. Current shunt sensors are used in precision current sources for feedback control systems. They are also used in a variety of other applications, including battery fuel gauging, laser diode power measurement and control, torque feedback controls in electric power steering, and precision power metering.

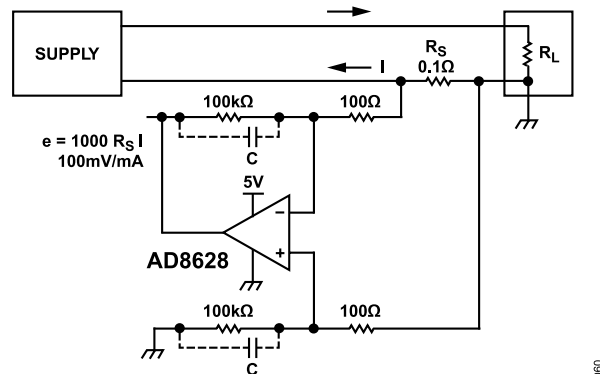


Figure 63. Low-Side Current Sensing

In such applications, it is desirable to use a shunt with very low resistance to minimize the series voltage drop; this minimizes wasted power and allows the measurement of high currents while saving power. A typical shunt might be 0.1 Ω. At measured current values of 1 A, the output signal of the shunt is hundreds of millivolts, or even volts, and amplifier error sources are not critical. However, at low measured current values in the 1 mA range, the 100 μV output voltage of the shunt demands a very low offset voltage and drift to maintain absolute accuracy. Low input bias currents are also needed, so that injected bias current does not become a significant percentage of the measured current. High open-loop gain, CMRR,

FUNCTIONAL DESCRIPTION

and PSRR help to maintain the overall circuit accuracy. As long as the rate of change of the current is not too fast, an auto-zero amplifier can be used with excellent results.

OUTPUT AMPLIFIER FOR HIGH PRECISION DACS

The AD8628/AD8629/AD8630 are used as output amplifiers for a 16-bit high precision DAC in a unipolar configuration. In this case, the selected op amp needs to have a very low offset voltage (the DAC LSB is 38 μV when operated with a 2.5 V reference) to eliminate the need for output offset trims. The input bias current (typically a few tens of picoamperes) must also be very low because it generates an additional zero code error when multiplied by the DAC output impedance (approximately 6 k Ω).

Rail-to-rail input and output provide full-scale output with very little error. The output impedance of the DAC is constant and code independent, but the high input impedance of the AD8628/AD8629/AD8630 minimizes gain errors. The wide bandwidth of the ampli-

ers also serves well in this case. The amplifiers, with settling time of 1 μs , add another time constant to the system, increasing the settling time of the output. The settling time of the AD5541 is 1 μs . The combined settling time is approximately 1.4 μs , as can be derived from the following equation:

$$t_s (TOTAL) = \sqrt{(t_s DAC)^2 + (t_s AD8628)^2} \quad (1)$$

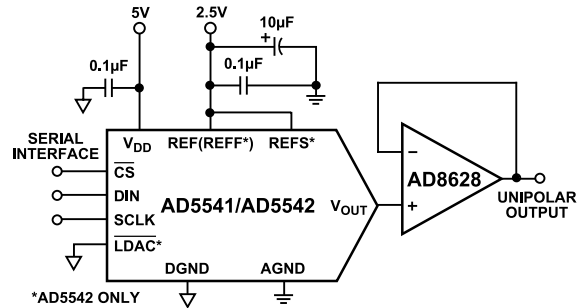
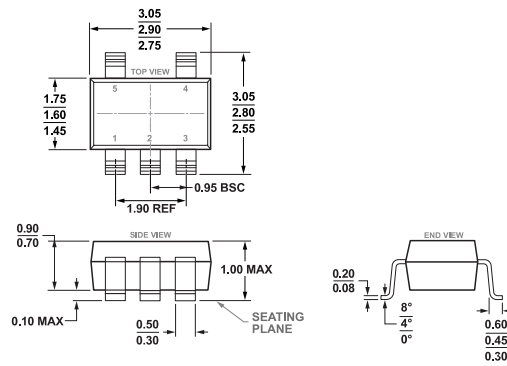


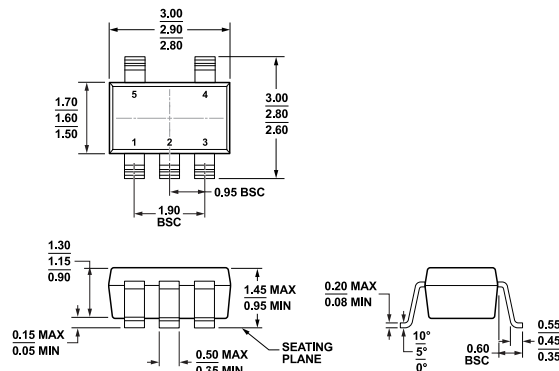
Figure 64. AD8628 Used as an Output Amplifier

OUTLINE DIMENSIONS



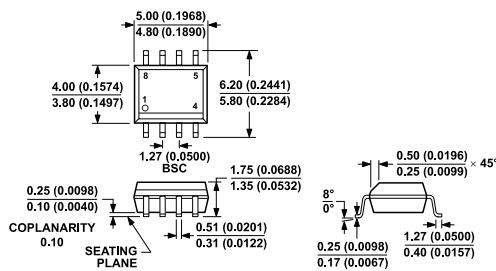
COMPLIANT TO JEDEC STANDARDS MO-193-AB

Figure 65. 5-Lead Thin Small Outline Transistor Package [TSOT] (UJ-5)
Dimensions shown in millimeters



COMPLIANT TO JEDEC STANDARDS MO-178-AA

Figure 66. 5-Lead Small Outline Transistor Package [SOT-23] (RJ-5)
Dimensions shown in millimeters



COMPLIANT TO JEDEC STANDARDS MS-012-AA

CONTROLLING DIMENSIONS ARE IN MILLIMETERS; INCH DIMENSIONS (IN PARENTHESES) ARE ROUNDED-OFF MILLIMETER EQUIVALENTS FOR REFERENCE ONLY AND ARE NOT APPROPRIATE FOR USE IN DESIGN.

Figure 67. 8-Lead Standard Small Outline Package [SOIC_N] Narrow Body (R-8)
Dimensions shown in millimeters and (inches)

OUTLINE DIMENSIONS

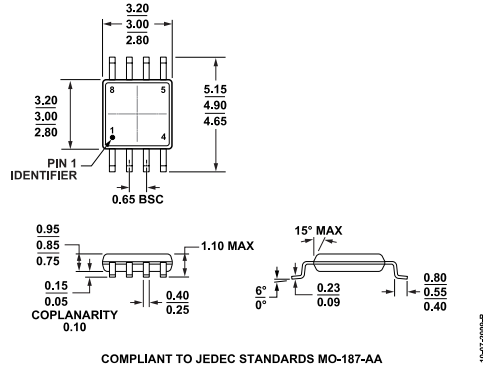


Figure 68. 8-Lead Mini Small Outline Package [MSOP] (RM-8)
Dimensions shown in millimeters

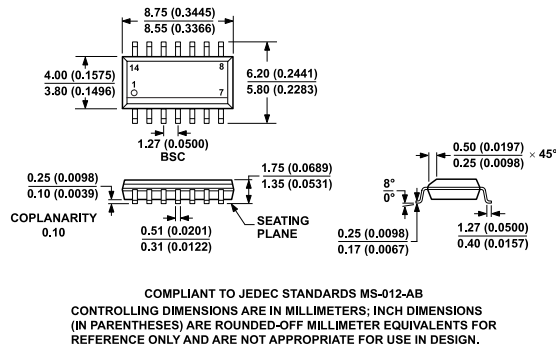


Figure 69. 14-Lead Standard Small Outline Package [SOIC_N] Narrow Body (R-14)
Dimensions shown in millimeters and (inches)

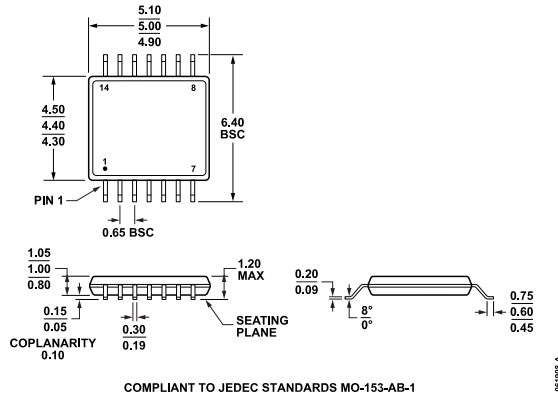


Figure 70. 14-Lead Thin Shrink Small Outline Package [TSSOP] (RU-14)
Dimensions shown in millimeters

Updated: September 20, 2022

ORDERING GUIDE

Model ^{1, 2}	Temperature Range	Package Description	Packing Quantity	Package Option	Marking Code
AD8628ARTZ-R2	-40°C to +125°C	5-Lead SOT-23	Reel, 250	RJ-5	AOL
AD8628ARTZ-REEL7	-40°C to +125°C	5-Lead SOT-23	Reel, 3000	RJ-5	AOL